

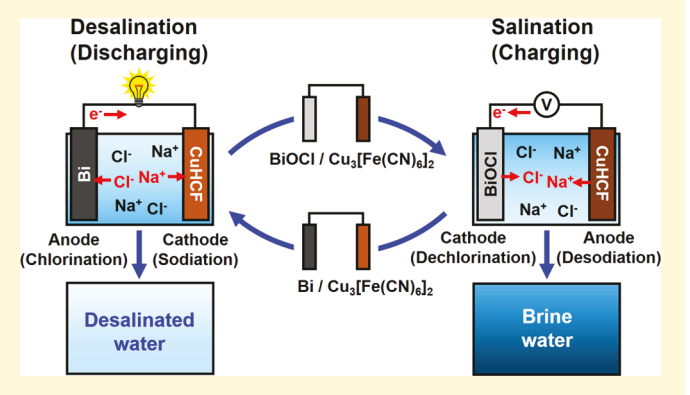
# A Desalination Battery Combining Cu<sub>3</sub>[Fe(CN)<sub>6</sub>]<sub>2</sub> as a Na-Storage Electrode and Bi as a Cl-Storage Electrode Enabling Membrane-Free **Desalination**

Do-Hwan Nam, Margaret A. Lumley, and Kyoung-Shin Choi\*

Department of Chemistry, University of Wisconsin-Madison, Madison, Wisconsin 53706, United States

Supporting Information

ABSTRACT: A desalination battery is an attractive route for seawater desalination because it couples ion removal with energy storage. In this work, we paired  $Cu_3[Fe(CN)_6]_2 \cdot nH_2O$ as the Na-storage electrode with Bi as the Cl-storage electrode to construct a novel desalination battery that enables membrane-free desalination. Most current desalination technologies, with the exception of thermal distillation, rely on the use of membranes. Eliminating the need for a membrane can significantly simplify the construction and maintenance of desalination systems. After carefully examining the sodiation/desodiation reactions and cycle performance of  $Cu_3[Fe(CN)_6]_2 \cdot nH_2O$  in both acidic and neutral saline solutions (0.6 M NaCl), we combined  $Cu_3[Fe(CN)_6]_2 \cdot nH_2O$ 



with Bi, which was previously identified as a promising Cl-storage electrode, to construct a Cu<sub>3</sub>[Fe(CN)<sub>6</sub>]<sub>2</sub>·nH<sub>2</sub>O/Bi desalination battery. The Cu<sub>3</sub>[Fe(CN)<sub>6</sub>]<sub>2</sub>·nH<sub>2</sub>O/Bi desalination battery generates an electrical energy output during desalination, which is equivalent to discharging, and requires an electrical energy input during salination, which is equivalent to charging. We investigated optimum pH conditions to perform salination to minimize the energy necessary for charging so that the desalination/salination cycle could be achieved with a minimum overall energy input. The results obtained in this study suggest that with further optimization the  $Cu_3[Fe(CN)_6]_2 \cdot nH_2O/Bi$  desalination battery will offer new possibilities for practical seawater desalination.

## ■ INTRODUCTION

Lack of access to fresh water is one of the most serious issues currently facing our society, 1-4 and seawater desalination is considered the most feasible approach to produce an adequate supply of fresh water. 5-8 Currently, thermal distillation and reverse osmosis (RO) are the two most established seawater desalination methods. <sup>6–10</sup> While RO is less energy intensive than thermal distillation, it still requires significant electrical energy input for the operation of high-pressure pumps. In addition, processes related to the prevention of membrane fouling (i.e., pre-treatments and post-treatments of water) keep the cost of seawater RO high.8-12

Recently, various electrochemical desalination methods have been reported. 13-34 The operating principles of these electrochemical desalination methods are fundamentally different from those of RO and thus provide diverse opportunities to advance desalination technologies. Among these systems, desalination batteries are particularly attractive because they couple desalination with energy storage.<sup>29-34</sup> Like other conventional batteries (e.g., Li-ion batteries), desalination batteries store and release energy during the charging and discharging processes. However, through combination of a Nastorage electrode and a Cl-storage electrode, the energy storage and release are coupled with the removal and release of Na<sup>+</sup>

and Cl-. Because the energy consumed during the charging process is at least partially recovered during the discharging process, desalination batteries can potentially achieve costefficient desalination with a much lower energy requirement than conventional desalination systems. Furthermore, as Na<sup>+</sup> and Cl<sup>-</sup> are stored in the bulk of the Na-storage and Cl-storage electrodes, not just in the electrical double layer of the electrodes as in the case of capacitive deionization, a high capacity for salt removal can be achieved.<sup>29-33</sup> As a result, desalination batteries may be used for seawater desalination as well as brackish water desalination. Another distinct advantage of desalination batteries is the possibility to achieve membranefree desalination. Currently, membranes are a key component of most existing desalination technologies. For example, RO requires a semipermeable membrane that passes only water molecules but not salt ions to achieve desalination. Electrodialysis, which is the most cost-effective method for brackish water desalination, 10,11 also requires ion selective membranes that pass only cations or anions. However, desalination batteries, which remove Na<sup>+</sup> and Cl<sup>-</sup> via ion-specific electrode

Received: January 8, 2019 Revised: January 22, 2019 Published: January 23, 2019

reactions (i.e., Na-storage and Cl-storage reactions), ideally do not require the use of a membrane. Thus, desalination batteries have the potential to achieve membrane-free desalination, eliminating processes and costs associated with membrane fouling and replacement.

One major barrier for the construction of desalination batteries was the identification of an efficient and practical Clstorage electrode. Although many possible Na-storage electrodes have already been identified and investigated for use in Naion batteries, 35 the identification of an appropriate Cl-storage electrode was more challenging. The earliest work on desalination batteries by Pasta et al. used Ag as the Cl-storage electrode, which was paired with MnO2 as the Na-storage electrode.<sup>29</sup> However, the authors pointed out that the high cost of Ag and poor conductivity of AgCl were the major limiting factors for constructing Ag-based desalination batteries.<sup>29</sup> More recently, we have discovered that Bi can serve as an effective and practical Cl-storage electrode based on the electrochemical conversion between Bi and BiOCl (eq 1).30 Successful operation of the first Bi-based desalination battery was demonstrated by coupling Bi as a Cl-storage electrode with NaTi<sub>2</sub>(PO<sub>4</sub>)<sub>3</sub> as a Na-storage electrode.

$$Bi + Cl^{-} + H_2O \rightleftharpoons BiOCl + 2H^{+} + 3e^{-}$$
 (1)

In this previous study, an undivided membrane-free cell was used for the desalination step, but a Nafion membrane was still required to divide the anode and cathode compartments during the salination step.<sup>30</sup> During the desalination reaction a neutral saline solution was used, but the overpotential required for the release of Cl from BiOCl during the salination reaction was found to be much lower in acidic solution and so an acidic solution was used for the salination reaction. The use of an acidic solution, however, was not compatible with the desodiation reaction of Na<sub>3</sub>Ti<sub>2</sub>(PO<sub>4</sub>)<sub>3</sub> because Na<sub>3</sub>Ti<sub>2</sub>(PO<sub>4</sub>)<sub>3</sub> is spontaneously oxidized in acidic solution, and discharge of Na<sup>+</sup> occurs. Therefore, the salination step of the Bi/ NaTi<sub>2</sub>(PO<sub>4</sub>)<sub>3</sub> battery required the use of a divided cell where the reduction of BiOCl was performed in an acidic solution while the oxidation of Na<sub>3</sub>Ti<sub>2</sub>(PO<sub>4</sub>)<sub>3</sub> was performed in a neutral solution. In other words, the role of the membrane in this desalination battery was simply to allow the Cl-release and Na-release reactions to be performed in two different pH conditions. Therefore, the identification of a Na-storage electrode that exhibits stability during sodiation in neutral solution and desodiation in acidic solution will enable the construction of a membrane-free Bi-based desalination battery.

In this study, we investigated the performance and stability of Cu<sub>3</sub>[Fe(CN)<sub>6</sub>]<sub>2</sub>·nH<sub>2</sub>O as a Na-storage electrode in both neutral and acidic solutions with the intention to construct a membrane-free Bi-based desalination battery. Hexacyanoferrate materials have previously demonstrated excellent cyclability for sodiation/desodiation reactions in acidic media.<sup>36-39</sup> However, for use in a desalination battery for seawater desalination, it is important to investigate the compatibility of  $Cu_3[Fe(CN)_6]_2 \cdot nH_2O$  with a neutral concentrated NaCl solution mimicking the composition of seawater. In addition, we needed to confirm that the presence of Cl would not affect the desodiation properties in acidic media. Therefore, we examined the sodiation/desodiation properties and cyclability of Cu<sub>3</sub>[Fe(CN)<sub>6</sub>]<sub>2</sub>·nH<sub>2</sub>O in both acidic and neutral 0.6 M NaCl solutions. Then, we constructed a membrane-free Cu<sub>3</sub>[Fe(CN)<sub>6</sub>]<sub>2</sub>·nH<sub>2</sub>O/Bi desalination battery and evaluated its performance for seawater desalination.

#### **■** EXPERIMENTAL SECTION

**Materials.** NaCl (99%, Macron), BiCl<sub>3</sub> (≥98%, Sigma-Aldrich), polyethylene glycol (PEG) (molecular weight of 6000, USB Corporation), HCl (37%, Sigma-Aldrich), CuSO<sub>4</sub>·SH<sub>2</sub>O (≥98%, Sigma-Aldrich), K<sub>3</sub>Fe(CN)<sub>6</sub> (≥95%, Mallinckrodt), polytetrafluoroethylene (PTFE) (60 wt % dispersion in H<sub>2</sub>O, Sigma-Aldrich), Super P Li (TimCal), and colloidal graphite (isopropanol, Ted Pella, Inc.) were used without further purification. Deionized water (Barnstead Epure water purification system, resistivity >18 MΩ·cm) was used to prepare all solutions.

Preparation of Cu<sub>3</sub>[Fe(CN)<sub>6</sub>]<sub>2</sub>·nH<sub>2</sub>O Electrodes. Cu<sub>3</sub>[Fe-(CN)<sub>6</sub>]<sub>2</sub>·nH<sub>2</sub>O was synthesized by a coprecipitation method following the procedure reported in a previous study.<sup>37</sup> First, 100 mL of 0.1 M CuSO<sub>4</sub>·5H<sub>2</sub>O and 100 mL of 0.05 M K<sub>3</sub>Fe(CN)<sub>6</sub> were added dropwise simultaneously to 60 mL of water while stirring at room temperature. A cloudy brown solution formed instantaneously upon mixing of the two reagents. The solution was then sonicated for 30 min and allowed to sit overnight (~12 h). The resulting precipitate was centrifuged at 5000 rpm and washed repeatedly with water until the washing solution was clear. The precipitate was then dried at 70 °C for 24 h in air. The product was ground with a mortar and pestle into a fine powder that was olive green in color. To prepare  $Cu_3[Fe(CN)_6]_2 \cdot nH_2O$  electrodes for testing,  $Cu_3[Fe(CN)_6]_2 \cdot nH_2O$ powder (0.2 g) was ground in a mortar and pestle with Super P Li (0.03 g) and a PTFE binder (0.02 g) with a ratio of 80:12:8 by mass using ethanol as the solvent. The paste that formed was kneaded and rolled into a sheet to prepare sheet-type electrodes with a thickness of  $\sim$ 120  $\mu$ m. The sheets were allowed to dry at 70 °C for 1 h to remove any residual ethanol. An electrode with an area of 1 cm<sup>2</sup> was punched from the sheet and attached onto a graphite current collector using colloidal graphite paste. The average mass of  $\text{Cu}_3[\text{Fe}(\text{CN})_6]_2 \cdot n \text{H}_2\text{O}$ in the electrodes was 0.02 g cm<sup>-2</sup>.

Preparation of Bi Foam Electrodes. Bi electrodes used in this study were prepared by electrodeposition following the procedure reported in our previous study.<sup>30</sup> An undivided three-electrode cell was used with a Ti sheet as the working electrode, a Pt sheet as the counter electrode, and a saturated calomel electrode (SCE) as the reference electrode. The Ti sheet was masked to expose an area of 1 cm<sup>2</sup>. An aqueous solution containing 14 mM BiCl<sub>3</sub>, 1.4 M HCl, and 2.5 g/L PEG 6000 was used as the plating solution. Potentiostatic deposition was performed by applying a potential of −2.6 V vs SCE for 2 min, resulting in the deposition of Bi (Bi<sup>3+</sup> + 3e<sup>-</sup>  $\rightarrow$  Bi,  $E^{\circ}$  = 0.286 V vs SHE). During the deposition, the solution was stirred at 300 rpm, and the average deposition current was ~900 mA cm<sup>-2</sup>. After deposition, the Bi electrodes were rinsed with water and dried in air. The average mass of Bi in the electrodes was  $\sim$ 1.25 mg cm<sup>-2</sup>. The Faradaic efficiency for Cl<sup>-</sup> removal and the milligrams of Cl<sup>-</sup> removed per gram of Bi were previously reported to be ~100% and 82.96  $mg_{Cl}/g_{Bi}$ , respectively.

**Characterization.** X-ray diffraction (XRD) patterns were collected using a Bruker D8 diffractometer with Ni-filtered Cu  $K\alpha$  radiation ( $\lambda$  = 1.5418 Å). The film morphology was examined using a LEO 1530 scanning electron microscope (SEM) operated at an accelerating voltage of 2 kV. Energy-dispersive X-ray spectroscopy (EDS) was performed using the same SEM equipped with an EDS (Noran System Seven, Thermo Fisher) at an accelerating voltage of 20 kV. Inductively coupled plasma optical emission spectrometry (ICP-OES) was performed to characterize the amount of Fe present in the solutions after the cycling tests (PerkinElmer Optima 2000).

**Electrochemical Testing.** Before assembling a  $Cu_3[Fe(CN)_6]_2 \cdot nH_2O/Bi$  desalination battery, we first examined the sodiation/desodiation performances of the  $Cu_3[Fe(CN)_6]_2 \cdot nH_2O$  electrode as half-cell reactions using an undivided three-electrode cell. A  $Cu_3[Fe(CN)_6]_2 \cdot nH_2O$  sheet was used as the working electrode (WE), Pt was used as the counter electrode (CE), and a double junction Ag/AgCl (4 M KCl) electrode was used as the reference electrode (RE). The Pt CE was prepared by sputter-coating a 100 nm thick Pt layer over a 20 nm thick Ti adhesion layer onto a clean glass slide (LGA Thin Films). The electrolyte (40 mL) was either neutral

0.6 M NaCl (pH 6.2, pH not adjusted) or acidic 0.6 M NaCl (pH adjusted to 1.2 with HCl). The distance between the WE and CE was less than 0.5 cm to minimize the IR drop from the solution. Galvanostatic sodiation/desodiation tests were performed where the  $Cu_3[Fe(CN)_6]_2 \cdot nH_2O$  electrodes were cycled at a current density of  $\pm 1.2$  mA cm<sup>-2</sup> (~1 C-rate if the theoretical specific capacity for  $Cu_3[Fe(CN)_6]_2 \cdot nH_2O$  is assumed to be ~60 mAh g<sup>-1</sup>) with cutoff potentials of 0.4 and 1.1 V vs Ag/AgCl for sodiation and desodiation, respectively. The change in Na<sup>+</sup> concentration in the electrolyte was measured using a sodium ion meter (Horiba B-722).

The desalination and salination performances of the Cu<sub>3</sub>[Fe-(CN)<sub>6</sub>]<sub>2</sub>·nH<sub>2</sub>O/Bi cell were investigated using an undivided cell galvanostatically cycled at  $\pm 1$  mA cm<sup>-2</sup>. The desalination process was performed in a neutral 0.6 M NaCl solution (pH 6.2), and the salination process was performed in 65 mM HCl (pH 1.2). The salination reaction was also performed in a neutral 0.6 M NaCl solution (pH 6.2) to compare the kinetics for salination in neutral and acidic solutions. During these tests, in addition to measuring the cell voltage between the Cu<sub>3</sub>[Fe(CN)<sub>6</sub>]<sub>2</sub>·nH<sub>2</sub>O and Bi electrodes as a function of capacity, the individual potentials of the Cu<sub>3</sub>[Fe(CN)<sub>6</sub>]<sub>2</sub>. nH2O and Bi electrodes against an Ag/AgCl reference electrode were monitored. The desalination process was performed until the cell voltage (potential difference between the Cu<sub>3</sub>[Fe(CN)<sub>6</sub>]<sub>2</sub>·nH<sub>2</sub>O and Bi electrodes) reached 0 V, and the salination process was performed until the cell voltage reached 2.15 V in neutral solution and 1.32 V in acidic solution. We note that the Coulombic efficiency of the Cu<sub>3</sub>[Fe(CN)<sub>6</sub>]<sub>2</sub>·nH<sub>2</sub>O/Bi cell is always slightly higher than 100%. This is because the measured capacity during the reduction of BiOCl to Bi (dechlorination) is slightly higher than that measured during the oxidation of Bi to BiOCl (chlorination) due to water reduction to H2 occurring as a side reaction during reduction. To prevent this from creating an issue during the desalination/salination cycling test, the Cu<sub>3</sub>[Fe(CN)<sub>6</sub>]<sub>2</sub>·nH<sub>2</sub>O electrode containing excess Cu<sub>3</sub>[Fe(CN)<sub>6</sub>]<sub>2</sub>· nH<sub>2</sub>O was prepared and was 50% pre-sodiated before the cycling test so that complete dechlorination of BiOCl would be achieved in each cycle. After each desalination or salination process was complete, the Cu<sub>3</sub>[Fe(CN)<sub>6</sub>]<sub>2</sub>·nH<sub>2</sub>O and Bi electrodes were manually lifted from the solution, rinsed with DI water, and moved into the next solution for the subsequent process.

# ■ RESULTS AND DISCUSSION

Synthesis and Characterization of  $\text{Cu}_3[\text{Fe}(\text{CN})_6]_2$ · $n\text{H}_2\text{O}$  (CuHCF) as a Na-Storage Material.  $\text{Cu}_3[\text{Fe}(\text{CN})_6]_2 \cdot n\text{H}_2\text{O}$  used in this study was prepared by a coprecipitation reaction in aqueous solution using  $\text{CuSO}_4$  and  $\text{K}_3\text{Fe}(\text{CN})_6$  precursors. As shown in Figure 1a, all peaks of the XRD pattern of the as-prepared sample were indexed and well matched with those of  $\text{Cu}_3[\text{Fe}(\text{CN})_6]_2$  (JCPDS #86-0513). Additionally, the atomic  $\text{Cu}_3[\text{Fe}(\text{CN})_6]_2$ · $n\text{H}_2\text{O}$ . The SEM images show that the as-synthesized  $\text{Cu}_3[\text{Fe}(\text{CN})_6]_2 \cdot n\text{H}_2\text{O}$  powder consists of micrometer-size particles (Figure 1b) composed of nanocubes with 100–200 nm long edges (Figure 1c).

Cu<sub>3</sub>[Fe(CN)<sub>6</sub>]<sub>2</sub>·nH<sub>2</sub>O is a Prussian blue analogue whose structure can be best described by comparison to an ABX<sub>3</sub> perovskite-type structure; B sites are occupied by alternating Cu(II) and Fe(III) ions, and X sites are occupied by CN groups (Figure 2).<sup>28,36,40,41</sup> The Cu(II) ions are octahedrally coordinated to the nitrogen ends of the CN groups and the Fe(III) ions are octahedrally coordinated to the carbon ends of the CN groups, creating a framework of -NC-Fe-CN-Cu-NC-linear linkages. When all B sites and X sites are occupied, 50% of the A sites are occupied by a monovalent ion, such as K<sup>+</sup>, to balance the charge, resulting in the formula KCu<sup>II</sup>Fe<sup>III</sup>CN<sub>6</sub>.<sup>41</sup>

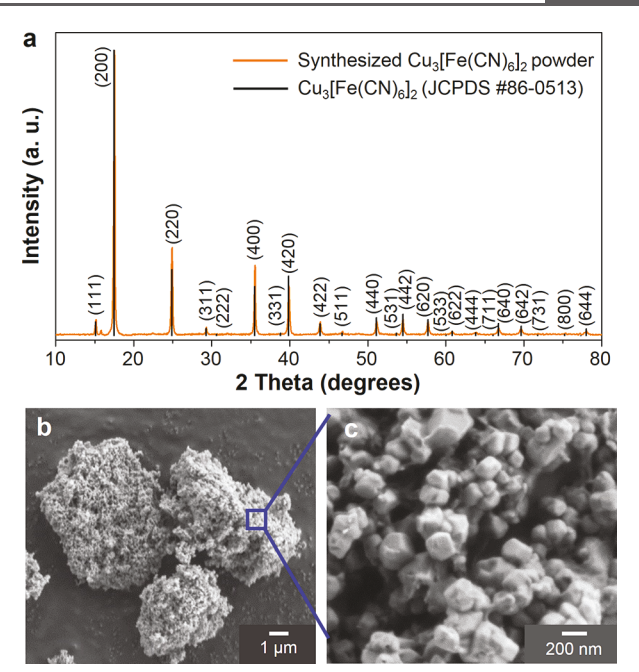
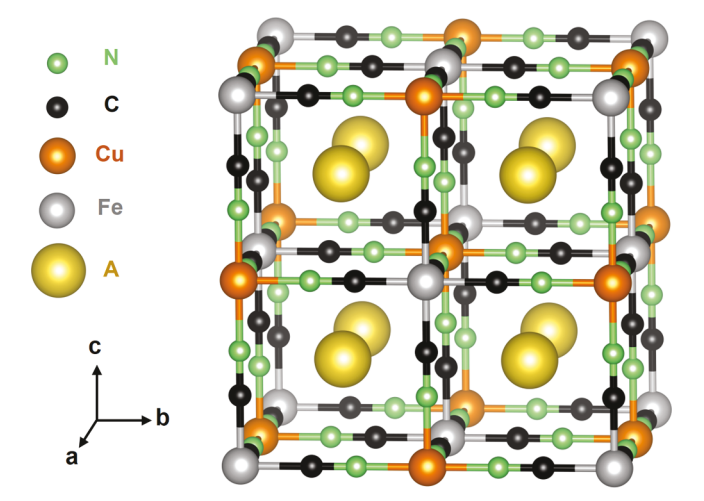


Figure 1. (a) XRD pattern and (b, c) SEM images of as-synthesized  $Cu_3[Fe(CN)_6]_2 \cdot nH_2O$  (CuHCF) powder.



**Figure 2.** Unit cell of a Prussian blue analogue with an  $ABX_3$  perovskite-type structure, where B sites are occupied by alternating Cu(II) and Fe(III) ions and X sites are occupied by CN groups. The degree of occupancy of the A site varies depending on the Cu(II)/Fe(III) ratio and the Fe(II)/Fe(III) ratio.

 ${\rm Cu_3[Fe(CN)_6]_2}\cdot n{\rm H_2O}$  prepared in this study, which is one of the readily formed copper hexacyanoferrate (CuHCF) phases, has 1/3 of the Fe(III) sites and 1/3 of the CN sites unoccupied. As a result, all A sites are also unoccupied to maintain charge neutrality. The vacant sites created by missing Fe ions and CN ions are occupied by water molecules. The water content of  ${\rm Cu_3[Fe(CN)_6]_2}\cdot n{\rm H_2O}$  has been reported to be  $\sim$ 5  ${\rm H_2O}$  molecules per one Fe atom, 40 but the exact water content can vary depending on the temperature and humidity. 36,37 For the rest of this study,  ${\rm Cu_3[Fe(CN)_6]_2}\cdot n{\rm H_2O}$  will be abbreviated as CuHCF.

CuHCF can act as a Na-storage material because the reduction of Fe(III) to Fe(II) in CuHCF can be coupled with the incorporation of  $Na^+$  into the A site to balance the charge (forward reaction of eq 2). Alternatively, when Fe(II) is

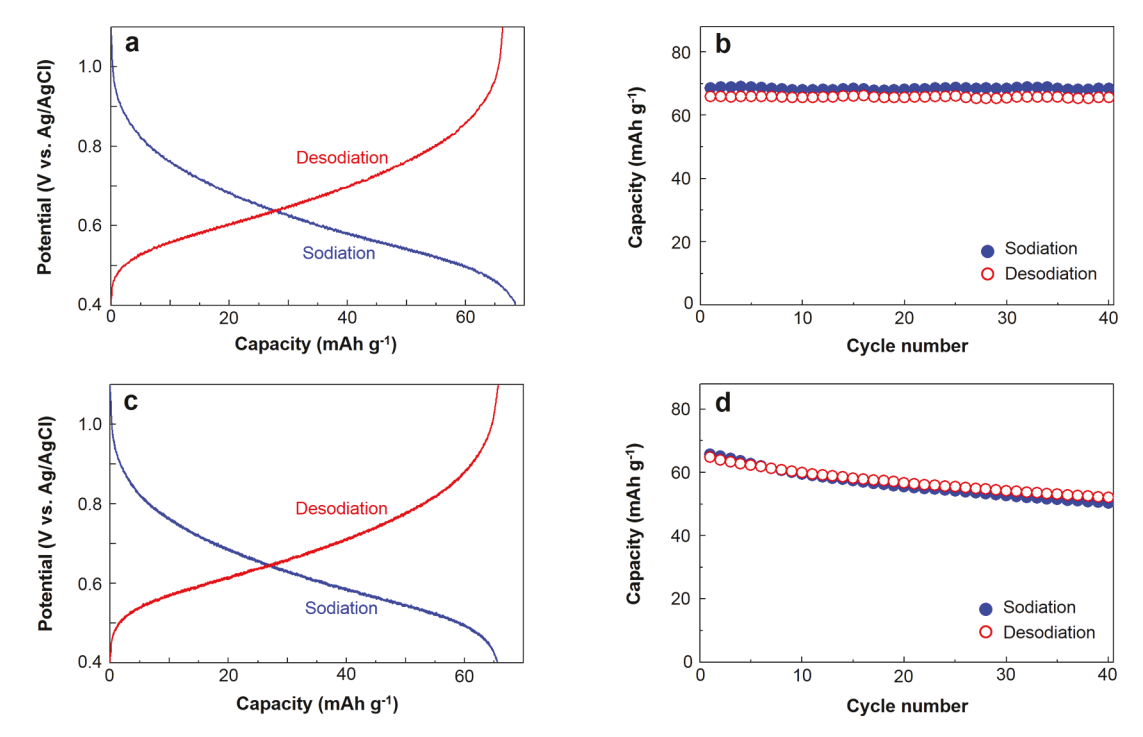


Figure 3. (a) Potential—capacity plots and (b) cycle performance of the CuHCF electrode tested at a current density of 60 mA g<sup>-1</sup> in an acidic 0.6 M NaCl solution (pH 1.2). (c) Potential—capacity plots and (d) cycle performance of the CuHCF electrode tested at a current density of 60 mA g<sup>-1</sup> in a neutral 0.6 M NaCl solution (pH 6.2).

oxidized, Na<sup>+</sup> is released and desodiation of CuHCF is achieved (reverse reaction of eq 2).

$$Cu_{3}[Fe^{III}(CN)_{6}]_{2} \cdot nH_{2}O + 2xNa^{+} + 2xe^{-}$$

$$\Rightarrow Na_{2x}Cu_{3}[Fe_{x}^{II}Fe_{1-x}^{III}(CN)_{6}]_{2} \cdot nH_{2}O$$
(2)

Before assembling a CuHCF/Bi desalination battery, the sodiation/desodiation performances of the CuHCF electrode were first examined as half-cell reactions using an undivided three-electrode setup where CuHCF was used as the WE with an Ag/AgCl (4 M KCl) RE and a Pt CE. The potentialcapacity plots were obtained in an acidic 0.6 M NaCl solution (pH 1.2, adjusted with HCl) at a current density of 60 mA g<sup>-1</sup> (rate of  $\sim 1$  C, equivalent to  $\sim 1.2$  mA cm<sup>-2</sup>). The electrode was cycled with cutoff potentials of 0.4 and 1.1 V vs Ag/AgCl for sodiation and desodiation, respectively (Figure 3a). A more detailed description of the experimental setup can be found in the Experimental Section. The C-rate was calculated based on previously reported capacities of ~60 mAh g<sup>-1</sup> because the theoretical capacity of CuHCF is difficult to calculate due to its hydrated form.<sup>36</sup> The gradually changing potential during the sodiation and desodiation processes indicates that the insertion/extraction of Na+ into/from CuHCF involves only a composition change of the same phase (i.e., formation of a solid solution). (If the sodiation/desodiation reaction resulted in the formation of a new phase instead of a solid solution, a plateau of the potential would have been observed instead. 42) Such a potential profile agrees well with the potential profiles that have been reported for other hexacyanoferrate-based Nastorage electrodes. 15-18,28,36-39

The CuHCF electrode showed excellent cycle stability with good capacity retention and Coulombic efficiency in acidic 0.6 M NaCl solution (Figure 3b). The first sodiation and desodiation capacities were 68.4 mAh g<sup>-1</sup> and 66.3 mAh g<sup>-1</sup>, respectively, giving a Coulombic efficiency of 97%. After 40

cycles, the sodiation capacity was maintained at 68.3 mAh g<sup>-1</sup>, corresponding to a capacity retention of 99.9%.

The sodiation/desodiation performances of CuHCF were also examined in neutral 0.6 M NaCl solution (pH 6.2) (Figure 3c). The potential-capacity plots in neutral solution looked comparable to those obtained in acidic solution, suggesting that the desodiation and sodiation reactions of CuHCF were not affected by increasing the pH from 1.2 to 6.2. Because the CuHCF/Bi desalination battery will perform desalination in a neutral solution, the ability of CuHCF to remove Na+ during sodiation in a neutral solution was quantified in terms of milligrams of Na<sup>+</sup> removed per gram of CuHCF using a sodium ion meter. Considering the sodiation capacity of 65.7 mAh g<sup>-1</sup> shown in Figure 3c and the mass of CuHCF in the CuHCF electrode (20 mg), 56.36 mg of Na<sup>+</sup> is expected to be removed per gram of CuHCF assuming 100% Faradaic efficiency (FE). The actual FE for Na<sup>+</sup> removal by CuHCF and milligrams of Na<sup>+</sup> removed per gram of CuHCF were determined to be 87% (Table S1) and 49.03  $mg_{Na}/g_{CuHCF}$ , respectively.

While the sodiation/desodiation profiles in acidic 0.6 M NaCl and neutral 0.6 M NaCl solutions were comparable, the cycle performance in neutral solution did not appear to be as good as that obtained in acidic solution. The initial sodiation capacity decreased from 65.7 to 50.0 mAh g<sup>-1</sup> after 40 cycles, corresponding to a capacity retention of only 76.1% (Figure 3d). After the cycling test in neutral 0.6 M NaCl solution, we observed a change in color of the solution from clear to fluorescent yellow, which was not observed after the cycling test in acidic 0.6 M NaCl solution (Figure 4a). The color of this solution resembled the color of a solution containing  $Fe(CN)_6^{3-}$ , suggesting that  $Fe(CN)_6^{3-}$  may have leached out from the CuHCF electrode during the cycling test in neutral solution. Indeed, ICP-OES analysis confirmed an increase in Fe content in the neutral 0.6 M NaCl solution from ~1 to ~15

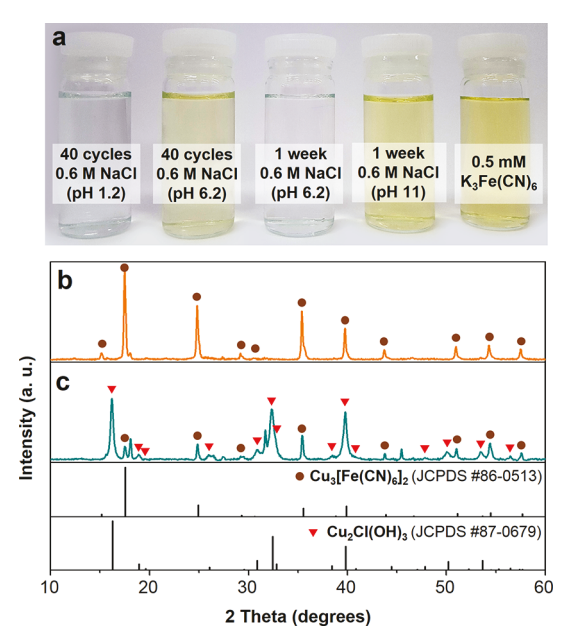


**Figure 4.** (a) Photographs showing the colors of the solutions after the cycling tests and chemical stability tests. The yellow color is due to the dissolution of  $\operatorname{Fe(CN)_6}^{3-}$ . XRD patterns of the CuHCF electrode after 40 cycles of sodiation/desodiation in (b) an acidic 0.6 M NaCl solution and (c) a neutral 0.6 M NaCl solution. The XRD patterns of  $\operatorname{Cu_3[Fe(CN)_6]_2} nH_2O$  and  $\operatorname{Cu_2Cl(OH)_3}$  are shown for reference.

mg/L after the cycling test. XRD patterns of the CuHCF electrode after the cycling test also showed that the CuHCF diffraction peaks diminished, and new peaks, which could all be assigned as peaks for  $\text{Cu}_2\text{Cl}(\text{OH})_3$ , appeared (Figure 4b,c). The ICP and XRD results suggest that during the cycling test  $\text{Fe}(\text{CN})_6^{3-}$  was lost from the CuHCF lattice, and the remaining copper formed  $\text{Cu}_2\text{Cl}(\text{OH})_3$  on the surface of the electrode.

To elucidate the cause of the instability of CuHCF, we first examined the solubility of CuHCF in a neutral 0.6 M NaCl solution but found no change in composition even after 1 week of immersion. However, when we increased the pH of the solution to 11, we visually observed the dissolution of  ${\rm Fe(CN)_6}^{3-}$  from CuHCF (Figure 4a and Figure S1) and saw the formation of  ${\rm Cu_2Cl(OH)_3}$  by XRD.

Indeed, CuHCF is known to decompose to  $Na_3Fe(CN)_6$  and CuO in the presence of NaOH through the following reaction:<sup>43</sup>

$$Cu_3[Fe(CN)_6]_2 + 6NaOH \rightarrow 2Na_3Fe(CN)_6 + 3CuO + 3H_2O$$
(3)

In the presence of Cl<sup>-</sup>, however,  $Cu_2Cl(OH)_3$ , rather than CuO, will form as one of the decomposition products (eq 4). We confirmed the thermodynamic feasibility of the formation of  $Cu_2Cl(OH)_3$  in 0.6 M NaCl solution by constructing a Pourbaix diagram for Cu in an aqueous solution containing 0.6 M Cl<sup>-</sup> (Figure S2). Based on these results, the degradation of CuHCF accompanied by the dissolution of  $Fe(CN)_6^{3-}$  that occurred during the cycling test in neutral saline water can be expressed as follows:

$$2Cu_{3}[Fe(CN)_{6}]_{2} \cdot nH_{2}O + 3CI^{-} + 9OH^{-}$$

$$\rightarrow 3Cu_{2}CI(OH)_{3} + 4Fe(CN)_{6}^{3-} + 2nH_{2}O$$
(4)

After elucidating that the instability of CuHCF was related to the reaction between CuHCF and OH<sup>-</sup>, we realized that the instability of CuHCF during the cycling test in neutral solution was caused by OH<sup>-</sup> generated from the Pt CE used in the three-electrode cell. The major reaction that can occur at the Pt CE in an aqueous solution during desodiation of the CuHCF electrode is water reduction (eq 5), which generates OH<sup>-</sup>.

$$2H_2O(1) + 2e^- \rightarrow H_2(g) + 2OH^-(aq)$$
 (5)

Because the CuHCF and Pt electrodes were kept very close (<0.5 cm) to minimize the IR drop from the solution, the local pH experienced by the CuHCF electrode could have increased significantly during water reduction at the Pt CE, resulting in the formation of  $Cu_2Cl(OH)_3$  and dissolution of  $Fe(CN)_6^{3-}$ . This also means that the capacity fading of the CuHCF electrode observed during the half-cell test in a neutral solution is not an intrinsic limitation of operating CuHCF in a neutral solution. Rather, it is a problem that arises from the alkaline pH generated from water reduction by the Pt CE that will not be used in a real device. Thus, when CuHCF is paired with an electrode/reaction that does not raise the pH to the alkaline region, CuHCF should not suffer from capacity fading. Therefore, we proceeded with the construction of a membrane-free CuHCF/Bi desalination battery. As we briefly explained in the Introduction, our aim is to operate the CuHCF/Bi battery in a neutral solution for desalination but in an acidic solution for salination because of the slow dechlorination kinetics of BiOCl in neutral solution. The Bi electrode will generate H<sup>+</sup> during chlorination in a neutral solution (eq 1), and the BiOCl electrode will generate OHduring dechlorination in an acidic solution. Because OH is generated only in an acidic solution where they can be readily neutralized by H+ in solution, degradation of CuHCF is not expected to be a problem during the operation of the CuHCF/ Bi battery.

Construction of a Membrane-Free CuHCF/Bi Desali**nation Battery.** After investigating the half-cell performances of CuHCF in neutral and acidic solutions, CuHCF was paired with Bi to fabricate a membrane-free desalination battery. A nanocrystalline Bi foam electrode was prepared by electrodeposition following the conditions reported in our previous study.<sup>30</sup> The deposition conditions were chosen such that Bi deposition and water reduction occurred simultaneously so that the H2 bubbles formed from water reduction could serve as an in situ template to create a Bi foam structure (Figure 5).30,44 The resulting electrode has a high interfacial area and can facilitate Cl<sup>-</sup> diffusion from the solution into the Bi lattice, enhancing the performance of Bi during chlorination. The XRD pattern of the Bi electrode used in this study is shown in Figure S3 and confirms the crystalline nature of the Bi foam. The detailed characterization and properties of Bi as a Clstorage electrode, which include SEM images and XRD patterns before and after chlorination and dechlorination, detailed electrochemical characterization, cycle tests, and Cl removal efficiency of the Bi electrodes, can be found in our previous study.<sup>30</sup>

The desalination performance of the CuHCF/Bi cell was first examined in a neutral 0.6 M NaCl solution galvanostatically cycled with a constant current density of 1 mA cm<sup>-2</sup>. During the desalination process, Fe(III) in CuHCF was reduced to Fe(II) to store Na<sup>+</sup> (cathode) while Bi was oxidized to BiOCl to store Cl<sup>-</sup> (anode). Therefore, electrons flowed

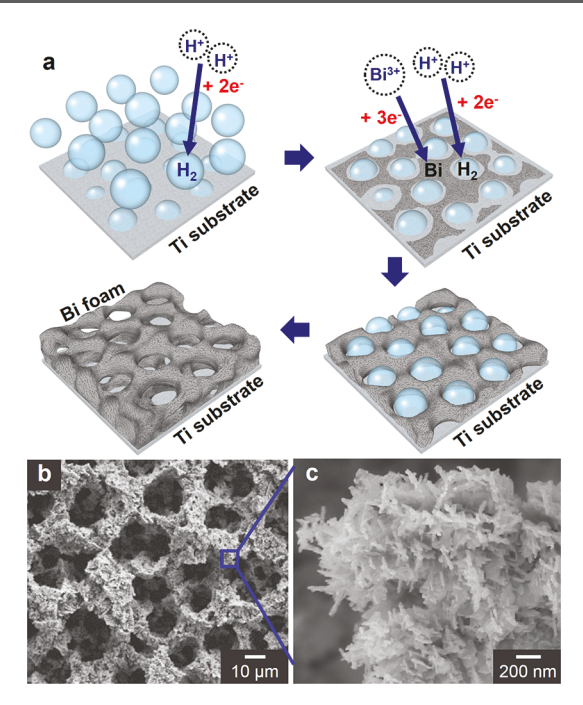


**Figure 5.** (a) Schematic illustration of the deposition of a Bi foam electrode using in situ generated  $H_2$  bubbles as a template and SEM images of a Bi foam electrode showing the (b) foam structure and (c) nanocrystalline Bi forming the foam wall.

from the Bi electrode to the CuHCF electrode. As the reaction proceeded, the potential of Bi rapidly increased from its open circuit potential and plateaued at -0.08 V vs Ag/AgCl while

the potential of the CuHCF electrode gradually decreased from 0.64 to 0.56 V vs Ag/AgCl (Figure 6a).

The cell potential  $(E_{\rm cell})$  of the CuHCF/Bi cell can be calculated by subtracting the anode potential  $(E_{\rm anode})$  from the cathode potential  $(E_{\rm cathode})$  using the equation  $E_{\rm cell} = E_{\rm cathode} - E_{\rm anode}$ . Because  $E_{\rm cathode}$  is more positive than  $E_{\rm anode}$  during the desalination reaction,  $E_{\rm cell}$  is positive. This means that for the CuHCF/Bi cell desalination is a spontaneous process equivalent to discharging, which generates electrical energy (Figure 7).

Figure 6b shows the potential profiles of the sodiated CuHCF and chlorinated Bi electrodes measured against the reference electrode during the salination process in neutral 0.6 M NaCl. During salination, the reduction of BiOCl and the oxidation of CuHCF occurred, and electrons flowed from the CuHCF electrode (anode) to the BiOCl electrode (cathode). As the reaction proceeded, the potential of the BiOCl electrode decreased from its open circuit potential and plateaued at around -1.15 V vs Ag/AgCl while the potential of the CuHCF electrode increased from 0.58 to 0.67 V vs Ag/ AgCl. Because the anode reaction (desodiation of CuHCF) occurs at a more positive potential than the cathode reaction (dechlorination of BiOCl),  $E_{cell}$  is negative. This means that salination performed by the CuHCF/Bi cell is a nonspontaneous process equivalent to charging and requires an energy input (Figure 7).

We note that the sodiation and desodiation potential profiles of CuHCF shown in Figures 6a and 6b are comparable. However, the chlorination and dechlorination potential profiles of Bi shown in Figures 6a and 6b are significantly different; the

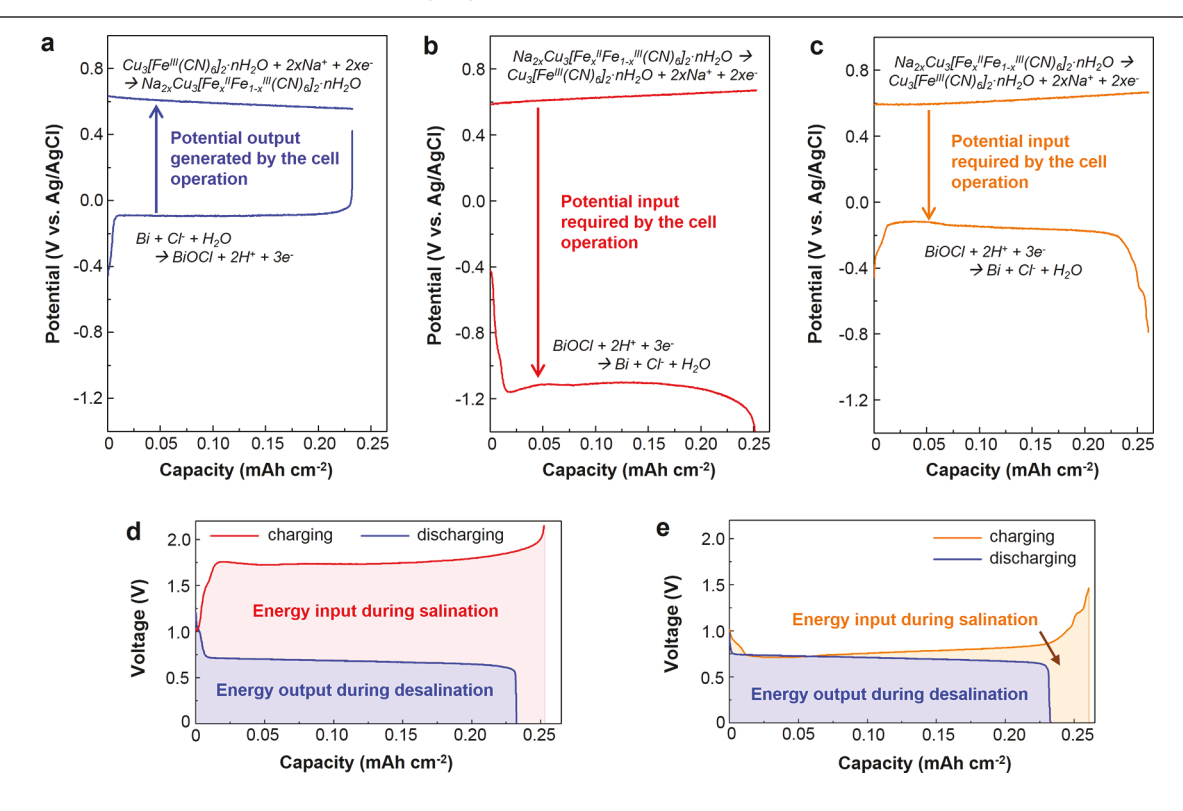
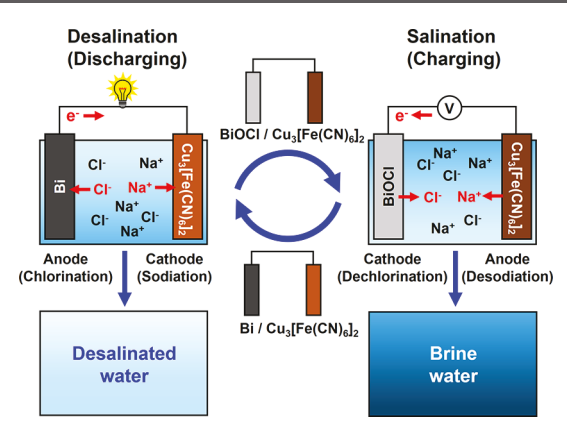


Figure 6. Potential—capacity plots for the CuHCF and Bi electrodes measured vs Ag/AgCl at a rate of  $\pm 1$  mA cm<sup>-2</sup> during (a) the desalination process in a neutral 0.6 M NaCl solution (pH 6.2), (b) the salination process in a neutral 0.6 M NaCl solution (pH 6.2), and (c) the salination process in 65 mM HCl (pH 1.2). Corresponding cell voltage—capacity plots (d) during discharging (desalination) in 0.6 M NaCl (pH 6.2) and charging (salination) in 0.6 M NaCl (pH 6.2) and charging (salination) in 0.6 M NaCl (pH 6.2) and charging (salination) in 65 mM HCl (pH 1.2).



**Figure 7.** Scheme showing the operation of the CuHCF/Bi desalination battery; the desalination process is equivalent to discharging and the salination process is equivalent to charging.

dechlorination of BiOCl occurred at a much more negative potential than the chlorination of Bi due to the slow kinetics of BiOCl reduction in neutral solution.<sup>30</sup> If the dechlorination potential of BiOCl can be moved closer to the chlorination potential of Bi, the cell potential required for salination can become more comparable to the cell potential generated during desalination, reducing the net energy requirement for the desalination/salination cycle.

In our previous study, we discovered that the kinetics for the dechlorination of BiOCl can be significantly improved when the solution is acidified. This is because the reduction of BiOCl to Bi involves the release of  $O^{2-}$  as well as  $Cl^-$  from the BiOCl lattice. In acidic media, protons in solution can serve as efficient  $O^{2-}$  acceptors and facilitate the reduction of BiOCl to Bi. Therefore, we also performed the salination process in 65 mM HCl (pH 1.2) to minimize the energy input required for salination. Because both BiOCl and CuHCF are stable in acidic solution, the salination reaction could be performed in an undivided cell, unlike the previous study where we coupled Bi with  $\rm Na_3Ti_2(PO_4)_3.^{30}$  We note that 65 mM HCl is used as an exemplary acidic medium. In real applications, any type of acidic wastewater with pH  $\sim 1$  can be used for the salination process.

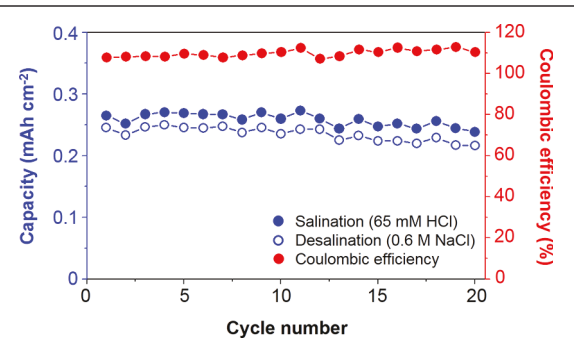
As shown in Figure 6c, when the charging process was performed in an acidic solution (pH 1.2), the average potential required for dechlorination of BiOCl was reduced from -1.15 to -0.15 V vs Ag/AgCl. The desodiation potential of CuHCF was comparable in both acidic and neutral 0.6 M NaCl solutions. As a result, the cell potential required for the salination process could be decreased significantly. We note that the equilibrium potential for the Bi/BiOCl reaction at pH 1.2 is -0.061 V vs Ag/AgCl while that at pH 6.2 is -0.28 V vs Ag/AgCl, which differ by only 0.21 V. Therefore, the majority of the decrease in cell potential observed in this study is due to a decrease in kinetic overpotential required for the conversion of BiOCl to Bi.

Figure 6d shows a comparison of cell potential—charge plots obtained when the desalination and salination processes were both performed in neutral 0.6 M NaCl solutions. The area below the desalination plot provides the energy output generated during discharging, and the area below the salination plot provides the energy input required during charging. (Note that the cell potential for the charging process, which is negative, is shown as positive in this plot for easy overlap of the integrated areas.) The difference between the energy generated

during desalination (0.158 mWh) and energy input required during salination (0.442 mWh) was calculated to be 0.284 mWh, which is the energy consumption required for a complete desalination/salination cycle. This means that 35.7% of the energy consumed during salination is recovered during desalination.

However, when salination was performed in 65 mM HCl (pH 1.2), the energy input required for salination was reduced from 0.442 to 0.209 mWh, resulting in a decrease in the overall energy consumption required for a desalination/salination cycle from 0.284 to 0.051 mWh (Figure 6e). In this case, 75.6% of the energy consumed during salination is recovered during desalination. A comparison between the energy consumption required for desalination by the CuHCF/Bi and Bi/NaTi<sub>2</sub>(PO<sub>4</sub>)<sub>3</sub> desalination batteries as well as that required for seawater reverse osmosis (SWRO) can be found in Table S2.

When the desalination and salination processes were repeated, the CuHCF/Bi cell showed relatively stable cycle performance over 20 cycles (Figure 8). The desalination



**Figure 8.** Cycling test of the CuHCF/Bi cell for desalination/salination. The discharging process (desalination) was performed in 0.6 M NaCl (pH 6.2), and the charging process (salination) was performed in 65 mM HCl (pH 1.2).

capacity was maintained at  $0.216 \text{ mAh cm}^{-2}$  after 20 cycles, corresponding to a retention of 87.8% of the initial desalination capacity ( $0.246 \text{ mAh cm}^{-2}$ ). The minor fluctuations in capacity shown during the cycling test are due to our experimental procedure, which involves manually lifting and immersing the CuHCF and Bi electrodes in two different solutions.

We note that the slight capacity fading observed during the cycling test is not due to the decomposition of CuHCF, which was easy to confirm as the solution did not change color, unlike what was observed during the half-cell test. We believe that this was caused by the pulverization of the Bi electrode due to the volume change involved during the conversion between Bi and BiOCl (158%). There are several effective strategies that can be used to improve the cycle performance of Bi, which include the addition of a carbon or polymer coating on Bi or making composites of Bi with Cl-inactive materials to buffer the volume change of Bi during chlorination/dechlorination. These strategies have been proven to work for the stabilization of other electrodes that suffer from this pulverization problem. 45,46 Because this study successfully confirmed the feasibility of constructing a membrane-free desalination battery using CuHCF and Bi electrodes, our future studies will focus on improving the long-term cyclability of the Bi electrode.

### CONCLUSION

In summary, we have demonstrated the successful fabrication of a CuHCF/Bi desalination battery that enables membranefree desalination. Before constructing the CuHCF/Bi desalination battery, we carefully examined the sodiation/desodiation performance and cyclability of CuHCF in both acidic and neutral 0.6 M NaCl solutions. CuHCF showed excellent cyclability for sodiation/desodiation in acidic 0.6 M NaCl solution. However, capacity fading was observed when neutral 0.6 M NaCl solution was used, which was caused by dissolution of Fe(CN)<sub>6</sub><sup>3-</sup> from the CuHCF lattice as evidenced by a yellow color change of the solution and the formation of Cu<sub>2</sub>Cl(OH)<sub>3</sub> on the electrode surface. We discovered that this instability was not due to any intrinsic limitation of CuHCF in neutral solution but due to a pH increase during the cycling test resulting from the counter electrode reaction (water reduction to H<sub>2</sub>). When CuHCF as a Na-storage electrode was paired with Bi as a Cl-storage electrode, the dissolution of Fe(CN)<sub>6</sub><sup>3-</sup> from CuHCF was no longer observed as the conversion between Bi and BiOCl does not cause an increase of the solution pH. The CuHCF/Bi desalination battery was tested for desalination in neutral 0.6 M NaCl while the test for salination was performed in both acidic and neutral conditions. For the CuHCF/Bi desalination battery, desalination was a discharging process, generating an energy output, and salination was a charging process, requiring an energy input. The use of an acidic solution for salination resulted in a significant decrease in the energy input required for charging, which became comparable to the energy output generated during desalination. As a result, the net energy consumption for the desalination/salination cycle could be minimized, successfully demonstrating the advantage of desalination batteries which couple salt removal with energy storage. Because both CuHCF and Bi are stable in neutral and acidic solutions, membranes were not necessary for the construction of this cell. The ability of the CuHCF/Bi battery to achieve desalination without the use of a membrane makes this device simple and unique. The CuHCF/Bi battery will provide a practical route for seawater desalination with further optimization of the cyclability of the Bi electrode.

## ASSOCIATED CONTENT

## S Supporting Information

The Supporting Information is available free of charge on the ACS Publications website at DOI: 10.1021/acs.chemmater.9b00084.

Photographs showing the pH-dependent dissolution of CuHCF, Pourbaix diagrams for Cu in the Cu $-H_2O$  and Cu $-Cl-H_2O$  systems, XRD patterns for the Bi foam electrode, Na removal efficiency, and energy requirement for desalination (PDF)

#### AUTHOR INFORMATION

## **Corresponding Author**

\*(K.-S.C.) E-mail: kschoi@chem.wisc.edu.

ORCID

Do-Hwan Nam: 0000-0002-5601-3172 Kyoung-Shin Choi: 0000-0003-1945-8794

#### Notes

The authors declare no competing financial interest.

### ACKNOWLEDGMENTS

This work was supported by the Wisconsin Alumni Research Foundation and the National Science Foundation (NSF) through Grant CBET-1803496.

## REFERENCES

- (1) Elimelech, M.; Phillip, W. A. The Future of Seawater Desalination: Energy, Technology, and the Environment. *Science* **2011**, 333, 712–717.
- (2) Shannon, M. A.; Bohn, P. W.; Elimelech, M.; Georgiadis, J. G.; Mariñas, B. J.; Mayes, A. M. Science and Technology for Water Purification in the Coming Decades. *Nature* **2008**, *452*, 301–310.
- (3) Mekonnen, M.; Hoekstra, A. Four Billion People Facing Severe Water Scarcity. Sci. Adv. 2016, 2, e1500323.
- (4) Cisneros, B. J. Water Recycling and Reuse: An Overview. In *Water Reclamation and Sustainability*; Ahuja, S., Ed.; San Diego, CA, 2014, pp 431–454.
- (5) Ghaffour, N.; Missimer, T. M.; Amy, G. L. Technical Review and Evaluation of the Economics of Water Desalination: Current and Future Challenges for Better Water Supply Sustainability. *Desalination* **2013**, 309, 197–207.
- (6) Ghaffour, N.; Bundschuh, J.; Mahmoudi, H.; Goosen, M. F. A. Renewable Energy-Driven Desalination Technologies: A Comprehensive Review on Challenges and Potential Applications of Integrated Systems. *Desalination* **2015**, *356*, 94–114.
- (7) Gude, V. G.; Nirmalakhandan, N.; Deng, N. S. Renewable and Sustainable Approaches for Desalination. *Renewable Sustainable Energy Rev.* **2010**, *14*, 2641–2654.
- (8) Burn, S.; Hoang, M.; Zarzo, D.; Olewniak, F.; Campos, E.; Bolto, B.; Barron, O. Desalination Techniques A Review of the Opportunities for Desalination in Agriculture. *Desalination* **2015**, 364, 2–16.
- (9) Missimer, T. M.; Maliva, R. G. Environmental Issues in Seawater Reverse Osmosis Desalination: Intakes and Outfalls. *Desalination* **2018**, 434, 198–215.
- (10) Saadat, A. H. M.; Islam, M. S.; Islam, M. S.; Parvin, F. Sultana, A. Desalination Technologies for Developing Countries: A review. *J. Sci. Res.* **2018**, *10*, 77–97.
- (11) Fritzmann, C.; Lowenberg, J.; Wintgens, T.; Melin, T. State-of-the-Art of Reverse Osmosis Desalination. *Desalination* **2007**, *216*, 1–76
- (12) Liu, Q.; Xu, G.-R. Graphene Oxide (GO) as Functional Material in Tailoring Polyamide Thin Film Composite (PA-TFC) Reverse Osmosis (RO) Membranes. *Desalination* **2016**, 394, 162–175
- (13) Nam, D.-H.; Choi, K.-S. Electrochemical Desalination Using Bi/BiOCl Electrodialysis Cells. ACS Sustainable Chem. Eng. 2018, 6, 15455–15462.
- (14) Smith, K. C.; Dmello, R. Na-Ion Desalination (NID) Enabled by Na-Blocking Membranes and Symmetric Na-Intercalation: Porous-Electrode Modeling. *J. Electrochem. Soc.* **2016**, *163*, A530–A539.
- (15) Smith, K. C. Theoretical Evaluation of Electrochemical Cell Architectures Using Cation Intercalation Electrodes for Desalination. *Electrochim. Acta* **2017**, 230, 333–341.
- (16) Porada, S.; Shrivastava, A.; Bukowska, P.; Biesheuvel, P. M.; Smith, K. C. Nickel Hexacyanoferrate Electrodes for Continuous Cation Intercalation Desalination of Brackish Water. *Electrochim. Acta* **2017**, *255*, 369–378.
- (17) Lee, J.; Kim, S.; Yoon, J. Rocking Chair Desalination Battery Based on Prussian Blue Electrodes. ACS Omega 2017, 2, 1653–1659.
- (18) Kim, T.; Gorski, C. A.; Logan, B. E. Low Energy Desalination Using Battery Electrode Deionization. *Environ. Sci. Technol. Lett.* **2017**, *4*, 444–449.
- (19) Jeon, S.- i.; Park, H.- r.; Yeo, J.-g.; Yang, S.; Cho, C. H.; Han, M. H.; Kim, D. K. Desalination Via a New Membrane Capacitive Deionization Process Utilizing Flow-Electrodes. *Energy Environ. Sci.* **2013**, *6*, 1471–1475.

(20) Jeon, S.- i.; Yeo, J.-g.; Yang, S.; Choi, J.; Kim, D. K. Ion Storage and Energy Recovery of a Flow-Electrode Capacitive Deionization Process. J. Mater. Chem. A 2014, 2, 6378–6383.

- (21) Cao, X.; Huang, X.; Liang, P.; Xiao, K.; Zhou, Y.; Zhang, X.; Logan, B. E. A New Method for Water Desalination Using Microbial Desalination Cells. *Environ. Sci. Technol.* **2009**, *43*, 7148–7152.
- (22) Srimuk, P.; Lee, J.; Tolosa, A.; Kim, C.; Aslan, M.; Presser, V. Titanium Disulfide: A Promising Low-Dimensional Electrode Material for Sodium Ion Intercalation for Seawater Desalination. *Chem. Mater.* **2017**, *29*, 9964–9973.
- (23) Desai, D.; Beh, E. S.; Sahu, S.; Vedharathinam, V.; van Overmeere, Q.; de Lannoy, C. F.; Jose, A. P.; Völkel, A. R.; Rivest, J. B. Electrochemical Desalination of Seawater and Hypersaline Brines with Coupled Electricity Storage. *ACS Energy Lett.* **2018**, *3*, 375–379.
- (24) Ma, B.; Chi, J.; Liu, H. Fabric-Based Ion Concentration Polarization for Pump-Free Water Desalination. *ACS Sustainable Chem. Eng.* **2018**, *6*, 99–103.
- (25) Kim, S.; Kim, C.; Lee, J.; Kim, S.; Lee, J.; Kim, J.; Yoon, J. Hybrid Electrochemical Desalination System Combined with an Oxidation Process. *ACS Sustainable Chem. Eng.* **2018**, *6*, 1620–1626.
- (26) Suss, M. E.; Presser, V. Water Desalination with Energy Storage Electrode Materials. *Joule* **2018**, *2*, 10–15.
- (27) Lee, J.; Kim, S.; Kim, C.; Yoon, J. Hybrid Capacitive Deionization to Enhance the Desalination Performance of Capacitive Techniques. *Energy Environ. Sci.* **2014**, *7*, 3683–3689.
- (28) Choi, S.; Chang, B.; Kim, S.; Lee, J.; Yoon, J.; Choi, J. W. Battery Electrode Materials with Omnivalent Cation Storage for Fast and Charge-Efficient Ion Removal of Asymmetric Capacitive Deionization. *Adv. Funct. Mater.* **2018**, *28*, 1802665.
- (29) Pasta, M.; Wessells, C. D.; Cui, Y.; La Mantia, F. A Desalination Battery. *Nano Lett.* **2012**, *12*, 839–843.
- (30) Nam, D.-H.; Choi, K.-S. Bismuth as a New Chloride-Storage Electrode Enabling the Construction of a Practical High Capacity Desalination Battery. *J. Am. Chem. Soc.* **2017**, *139*, 11055–11063.
- (31) Chen, F.; Huang, Y.; Guo, L.; Sun, L.; Wang, Y.; Yang, H. Y. Dual-Ions Electrochemical Deionization: A Desalination Generator. *Energy Environ. Sci.* **2017**, *10*, 2081–2089.
- (32) Chen, F.; Huang, Y.; Guo, L.; Ding, M.; Yang, H. Y. A Dual-Ion Electrochemistry Deionization System Based on AgCl-Na<sub>0.44</sub>MnO<sub>2</sub> Electrodes. *Nanoscale* **2017**, *9*, 10101–10108.
- (33) Chen, F.; Huang, Y.; Kong, D.; Ding, M.; Huang, S.; Yang, H. Y. NaTi<sub>2</sub>(PO<sub>4</sub>)<sub>3</sub>-Ag Electrodes Based Desalination Battery and Energy Recovery. *FlatChem.* **2018**, *8*, 9–16.
- (34) Srimuk, P.; Halim, J.; Lee, J.; Tao, Q.; Rosen, J.; Presser, V. Two-Dimensional Molybdenum Carbide (MXene) with Divacancy Ordering for Brackish and Seawater Desalination via Cation and Anion Intercalation. ACS Sustainable Chem. Eng. 2018, 6, 3739–3747.
- (35) Kim, H.; Hong, J.; Park, K.-Y.; Kim, H.; Kim, S.-W.; Kang, K. Aqueous Rechargeable Li and Na ion batteries. *Chem. Rev.* **2014**, *114*, 11788–11827.
- (36) Wessells, C. D.; Peddada, S. V.; Huggins, R. A.; Cui, Y. Nickel Hexacyanoferrate Nanoparticle Electrodes For Aqueous Sodium and Potassium Ion Batteries. *Nano Lett.* **2011**, *11*, 5421–5425.
- (37) Wessells, C. D.; Huggins, R. A.; Cui, Y. Copper Hexacyanoferrate Battery Electrodes with Long Cycle Life and High Power. *Nat. Commun.* **2011**, *2*, 550.
- (38) Paolella, A.; Faure, C.; timoshevskii, V.; Marras, S.; Bertoni, G.; Guerfi, A.; Vijh, A.; Armand, M.; Zaghib, K. A Review on Hexacyanoferrate-Based Materials for Energy Storage and Smart Windows: Challenges and Perspectives. *J. Mater. Chem. A* **2017**, *5*, 18919–18932.
- (39) Huggins, R. A. Review A New Class of High Rate, Long Cycle Life, Aqueous Electrolyte Battery Electrodes. *J. Electrochem. Soc.* **2017**, *164*, A5031–A5036.
- (40) Ayrault, S.; Jimenez, B.; Garnier, E.; Fedoroff, M.; Jones, D. J.; Loos-Neskovic, C. Sorption Mechanisms of Cesium on Cu<sup>II</sup><sub>2</sub>Fe<sup>II</sup>(CN)<sub>6</sub> and Cu<sup>II</sup><sub>3</sub>[Fe<sup>III</sup>(CN)<sub>6</sub>]<sub>2</sub> Hexacyanoferrates and Their Relation to the Crystalline Structure. *J. Solid State Chem.* **1998**, *141*, 475–485.

- (41) Ojwang, D. O.; Grins, J.; Wardecki, D.; Valvo, M.; Renman, V.; Häggström, L.; Ericsson, T.; Gustafsson, T.; Mahmoud, A.; Hermann, R. P.; Svensson, G. Structure Characterization and Properties of K-Containing Copper Hexacyanoferrate. *Inorg. Chem.* **2016**, *55*, 5924–5934
- (42) Nam, D.-H.; Kim, T.-H.; Hong, K.-S.; Kwon, H.-S. Template-Free Electrochemical Synthesis of Sn Nanofibers as High-Performance Anode Materials for Na-Ion Batteries. *ACS Nano* **2014**, *8*, 11824–11835.
- (43) Marshall, J. A Brief Introduction to Qualitative Analysis, for Use in Instruction in Chemical Laboratories, 6th ed.; J. B. Lippincott & Co.: Philadelphia, PA, 1906.
- (44) Nam, D. H.; Kim, R. H.; Han, D. W.; Kwon, H. S. Electrochemical Performances of Sn Anode Electrodeposited on Porous Cu foam for Li-ion Batteries. *Electrochim. Acta* **2012**, *66*, 126–132
- (45) Mahmood, N.; Tang, T.; Hou, Y. Nanostructured Anode Materials for Lithium Ion Batteries: Progress, Challenge and Perspective. *Adv. Energy. Mater.* **2016**, *6*, 1600374.
- (46) Kang, H.; Liu, Y.; Cao, K.; Zhao, Y.; Jiao, L.; Wang, Y.; Yuan, H. Update on Anode Materials for Na-Ion Batteries. *J. Mater. Chem. A* **2015**, *3*, 17899–17913.
- (47) Beverskog, B.; Puigdomenech, I. Pourbaix Diagrams for the System Copper-Chlorine at 5–100 °C. SKI (Swedish Nuclear Power Inspectorate) Rapport, 1998, 98:19, 1.
- (48) Voutchkov, N. Energy Use for Membrane Seawater Desalination. *Desalination* 2018, 431, 2-14.